IET Communications

Research Article

IET Journals
The Institution of Engineering and Technology

Comparison of adaptive algorithms for free space optical transmission in Málaga atmospheric turbulence channel with pointing errors

ISSN 1751-8628
Received on 11th July 2018
Revised 28th February 2019
Accepted on 25th March 2019
E-First on 17th May 2019
doi: 10.1049/iet-com.2018.5666
www.ietdl.org

Marko Smilić[1] ✉, *Zorica Nikolić*[2], *Dejan Milić*[2], *Petar Spalević*[3], *Stefan Panić*[4]

[1]*University of Priština, Faculty of Natural Sciences and Mathematics, Lole Ribara 29, Kosovska Mitrovica, Serbia*
[2]*University of Niš, Faculty of Electronic Engineering, Aleksandra Medvedeva 14, Niš, Serbia*
[3]*University of Priština, Faculty of Technical Sciences, Kneza Miloša 7, Kosovska Mitrovica, Serbia*
[4]*National Research Tomsk Polytechnic University, Sovetskaya 84/3, Tomsk, Russia*
✉ *E-mail: marko.smilic@pr.ac.rs*

Abstract: In this study, the authors investigate average capacity of free space optics communication over Málaga atmospheric turbulence channel with pointing errors and path loss, for intensity modulated/direct detection (IM/DD) and heterodyne detection. Various algorithms which use adaptive transmission with both types of detection are considered, such as: optimal rate adaption (ORA), optimal power and rate adaption (OPRA), channel inversion with fixed rate (CIFR) and truncated channel inversion with fixed rate (TIFR). Analytical closed-form expressions for channel capacities of ORA, OPRA and TIFR adaptive transmission are presented, and the authors prove that CIFR transmission is not feasible in the strict sense for the conditions considered. Obtained analytical results are numerically evaluated and graphically presented for different strengths of atmospheric turbulence (in weak, moderate and strong turbulence regime) for both types of detection (IM/DD and heterodyne), and for considered algorithms of adaptive transmission (ORA, OPRA and TIFR). The authors have developed expressions suitable for approximating high signal-to-noise ratio channel capacity, and they graphically present and compare the asymptotic approximations with the obtained analytical results for different strengths of turbulence for both types of detection. Also, obtained analytical results were confirmed by Monte-Carlo simulations, and graphically compared for different strengths of turbulence regimes.

1 Introduction

The study of wireless optical systems is generally a multidisciplinary undertaking involving a wide range of areas including: optical design, optoelectronics, channel modelling, communications and information theory, modulation and equalisation, wireless optical network architectures among many others [1]. The transport capabilities of optical communication systems have increased tremendously in the past two decades, primarily due to advances in optical devices and technologies, and have enabled the Internet as we know it today with all its impacts on the modern society [2].

Free space optics (FSO) links are considered as a viable solution for various applications because of the following properties [2–4]:

- the high-directivity of the optical beam provides high power efficiency and spatial isolation from other potential interferers, which is not inherent in RF/microwave communications,
- FSO transmission is unlicensed,
- the large fractional-bandwidth coupled with high optical gain using moderate powers permits very high data rate transmission,
- FSO links are relatively easy to install and easily accessible for repositioning when necessary.

Channel capacity is a fundamental measure of the maximum amount of information which can be conveyed through a channel reliably. Shannon's discovery that it was possible to have arbitrarily reliable communication at non-zero rates revolutionised communication system design practices and established the areas of information theory and error control coding [1, 5]. The capacity depends on the specific channel model and on the given input constraints [2].

Unlike RF communication, FSO requires a direct line of sight between the transmitter and the receiver. Atmospheric effects, such as rain, snow and fog, will affect the FSO link performance by means of scattering and absorption of light, effectively attenuating the received signal. During transmission, the transmitted FSO signal is also exposed to various effects such as atmospheric turbulence and misalignment between the transmitter and receiver (pointing error). The impact of these effects on free space optical system performance are explained in [6–8]. One of the more effective ways to reduce the impact of these detrimental effects is the use of adaptive transmission. Adaptive transmission is based on the receiver's estimation of the channel and feedback of the channel state information to the transmitter. The transmitter then adapts the transmit power level, symbol/bit rate, constellation size, coding rate/algorithms or any combination of these parameters in response to the changing channel conditions [9].

Málaga model represents a general model of atmospheric turbulence [10], covering other less general models such as K turbulence model, HK turbulence model, gamma and gamma-gamma turbulence models, exponential-Weibull turbulence models and so on. System performance for outage probability (P_{out}), symbol error rate, bit error rate (BER) over Málaga atmospheric turbulence channel are given in [11–13]. Also, BER for different modulation schemes over Málaga atmospheric turbulence model is presented in [14]. Diversity is a widely used and efficient technique for improving performance of communication systems. System performance for outage probability and BER when using different diversity techniques are given in [15–18].

Channel capacity represents one of the most important system performance measures. Ergodic capacity for lognormal, Rician-lognormal, Málaga and gamma-gamma atmospheric turbulence channel are given in [13, 19, 20]. Average capacity of optical wireless communication systems over I-K atmospheric turbulence channels without pointing error is given in [21]. Channel capacity

© The Institution of Engineering and Technology 2019

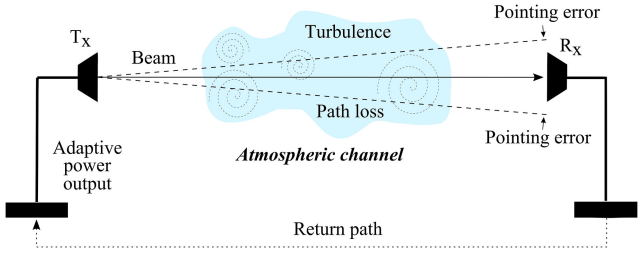

Fig. 1 *Model of FSO communication system with adaptive transmission*

for different atmospheric turbulence strengths is investigated in [22]. Capacity analysis of atmospheric turbulence channel with pointing errors is presented in [23]. Algorithms for adaptive transmission over gamma-gamma atmospheric turbulence channel are explained in [24–26].

It is worthy to note that intensity modulation/direct detection (IM/DD) is the main mode of detection in FSO systems, but coherent detection has also been proposed as an alternative detection mode. Among the two detection types, heterodyne coherent detection represents a method that is more complicated, but has the ability to better overcome the receiver thermal noise effects [13, 27], and therefore achieve better performance.

Motivated by this short review of existing results, we proceed to investigate average capacity of FSO communication over Málaga atmospheric turbulence channel with pointing error and path loss for both proposed types of detection, IM/DD and heterodyne. Also, various algorithms for adaptive transmission, such as: constant power rate adaption (ORA), optimal power rate adaption (OPRA), channel inversion with fixed rate (CIFR) and truncated channel inversion with fixed rate (TIFR) for both types of detection will be considered. Analytical closed-form expressions for ORA, OPRA and TIFR adaptive transmission algorithms will be derived. Obtained results are confirmed by Monte-Carlo simulations, and are further discussed for different turbulence strengths and types of detection. Also, we derive asymptotic high signal-to-noise ratio (SNR) approximations for channel capacity expressions and compare them graphically with analytical results.

2 System model

We consider an FSO system with constant transmitted power than can be adjusted according to adaptive transmission requirements. During transmission, the transmitted signal is exposed to various effects such as: atmospheric turbulence, scintillation, misalignment between the transmitter (T_x) and receiver (R_x), i.e. pointing error, and path loss, as shown in Fig. 1. All of these effects affect the system performance. To maintain a target data rate, the received SNR should not be less than a predetermined cut-off level denoted by g_0. When the current SNR at the receiver of the FSO link, denoted by g, falls below the cut-off level g_0, the FSO link cannot support the high data rate transmission. In this case, the receiver sends a feedback signal to the transmitter so that the transmitter increases its power and thus maintains the reliability of the link.

2.1 Atmospheric turbulence model

Málaga model represents a general model of atmospheric turbulence [10]. In this paper, we consider the case of Málaga atmospheric turbulence model with integer β [11], which can be expressed as

$$f_a(I_a) = A\sum_{k=1}^{\beta} a_k I_a^{\frac{\alpha+k}{2}-1} K_{\alpha-k}\left(2\sqrt{\frac{\alpha\beta I_a}{\gamma\beta+\Omega'}}\right) \tag{1}$$

where

$$A \triangleq \frac{2\alpha^{\frac{\alpha}{2}}}{\gamma^{1+\frac{\alpha}{2}}\Gamma(\alpha)}\left(\frac{\gamma\beta}{\gamma\beta+\Omega'}\right)^{\beta+\frac{\alpha}{2}} \tag{2}$$

$$a_k \triangleq \binom{\beta-1}{k-1}\frac{(\gamma\beta+\Omega')^{1-\frac{k}{2}}}{(k-1)!}\left(\frac{\Omega'}{\gamma}\right)^{k-1}\left(\frac{\alpha}{\beta}\right)^{\frac{k}{2}} \tag{3}$$

There is also the case of Málaga atmospheric turbulence model with real β [12], but it will not be considered here. Parameters α and β represent the effective numbers of large-scale and small-scale cells, respectively, and can be related to the atmospheric conditions. The parameters are expressed as

$$\alpha = \left(\exp\left[\frac{0.49\sigma_R^2}{\left(1+1.11\sigma_R^{12/5}\right)^{7/6}}\right]-1\right)^{-1} \tag{4}$$

$$\beta = \left(\exp\left[\frac{0.51\sigma_R^2}{\left(1+0.69\sigma_R^{12/5}\right)^{5/6}}\right]-1\right)^{-1} \tag{5}$$

where plane wave propagation and zero inner scale is assumed [28]. $\gamma = 2b_0(1-\rho)$ denotes the average power of the scattering component received by off-axis eddies, $2b_0$ is the average power of the total scatter components, parameter $0 \le \rho \le 1$ represents the amount of scattering power coupled to the line-of-sight (LOS) component, $\Omega' = \Omega + 2b_0\rho + 2\sqrt{2b_0\rho\Omega}\cos(\theta_A - \theta_B)$ symbolises the average power through the coherent advantages, Ω is the regular power of the LOS aspect, $(\theta_A - \theta_B)$ are the deterministic levels of the LOS and also the coupled-to-LOS spread terms, respectively [11]. σ_R^2 represents the Rytov variance and is used as a metric of turbulence strength. It is expressed by

$$\sigma_R^2 = 1.23C_n^2k^{7/6}L^{11/6} \tag{6}$$

where $k = 2\pi/\lambda$ is the wave number, λ is the wavelength, L is the propagation distance and C_n^2 is the refractive index structure parameter, which typically varies from $10^{-17}m^{-2/3}$ to $10^{-13}m^{-2/3}$ as turbulence strength varies from weak to strong [29].

2.2 Path loss

Path loss, I_l, can be described by the exponential Beers-Lambert laws as

$$I_l(L) = e^{-\sigma L} \tag{7}$$

where L denotes the propagation distance and σ is the attenuation coefficient.

2.3 Pointing error

Pointing errors also affect the transmission performance. In case of zero boresight pointing error, I_p, the following model is used [1]:

$$f_{I_p}(I_p) = \frac{\xi^2}{A_0^{\xi^2}}I_p^{\xi^2-1}, \qquad 0 \le I_p \le A_0 \tag{8}$$

where $\xi = \omega_{L_{eq}}/2\sigma_s$ is the ratio between the equivalent beam radius at the receiver $\omega_{L_{eq}}$ and the pointing error displacement standard deviation at the receiver σ_s. $A_0 = (\mathrm{erf}(v))^2$ is the fraction of the collected power where $v = \sqrt{\pi}a/\sqrt{2}\omega_{L_{eq}}$ with $\mathrm{erf}(\cdot)$ denoting the error function, where as the square of the equivalent beam width is given by

$$\omega_{L_{eq}}^2 = \omega_L^2\frac{\sqrt{\pi}\,\mathrm{erf}(v)}{2ve^{-v^2}} \tag{9}$$

3 Probability density function (PDF)

Combining the atmospheric turbulence model, pointing error and path loss, we get PDF of instantaneous SNR at the receiver for IM/DD and heterodyne detection. Closed-form expression for PDF

© The Institution of Engineering and Technology 2019

for Málaga atmospheric turbulence model with pointing error and path loss is given in [13] for integer β

$$f_g(g) = \frac{\xi^2 A}{2^r g}\sum_{k=1}^{\beta} a_k\left(\frac{\gamma\beta+\Omega'}{\alpha\beta}\right)^{\frac{\alpha+k}{2}} \times G_{1,3}^{3,0}\left(\eta(g)^{\frac{1}{r}}\middle|\begin{matrix}\xi^2+1\\ \xi^2,\alpha,k\end{matrix}\right) \tag{10}$$

where

$$\eta = \frac{\alpha\beta\kappa(\gamma+\Omega')}{(c\mu)^{\frac{1}{r}}(\gamma\beta+\Omega')} \tag{11}$$

Parameter r determines the type of detection technique ($r = 1$ for heterodyne detection and $r = 2$ for IM/DD) and c denotes a constant term such that $c = 1$ for heterodyne detection and $c = e/2\pi$ for IM/DD [13]. The received instantaneous SNR is defined as

$$g = \frac{(2P_t RI)^2}{2\sigma_n^2} \tag{12}$$

where σ_n^2 denotes additive white Gaussian noise, and I represents the irradiance $I = I_a I_l I_p$. Average electrical SNR can be defined as

$$\mu = \frac{(2P_t R)^2}{2\sigma_n^2}\mathrm{E}[I^2] \tag{13}$$

where $E[.]$ is the statistical expectation. Average electrical SNR from equation (13) can be determined as [30]

$$\mu = \frac{(2P_t R)^2}{2\sigma_n^2} A_0^2 I_l^2 \kappa^2(\gamma+\Omega')^2 \tag{14}$$

4 Channel capacity

Channel capacity is one of the most important concerns in the design of wireless systems, as it determines the maximum attainable throughput of the system. It can be defined as the average transmitted data rate per unit bandwidth, for a specified average transmit power, and specified level of received outage or BER [31].

Adaptive transmission techniques represent a viable solution for reducing the influence of atmospheric turbulence, misalignment and path loss to propagation of transmitted signal. This is achieved by adapting basic parameters of the transmitted signal. The main advantage of the adaptive transmission is that it provides opportunity to attain higher spectral efficiency within the channel bandwidth.

In this section, capacity for various adaptive transmission algorithms (ORA, OPRA, CIFR and TIFR) will be derived. Analytical expressions in closed-form will be given for proposed algorithms with IM/DD and heterodyne detection.

4.1 Optimal rate adaption

With ORA algorithm, the transmitter adapts its rate only, while maintaining a fixed power level. Thus, this algorithm can be implemented at reduced complexity. Channel capacity $\langle C\rangle_{\mathrm{ora}}$ [bits/s] with constant transmission power policy is given by [31]

$$\langle C\rangle_{\mathrm{ora}} = B\int_0^{\infty}\log_2(1+g)f_g(g)\mathrm{d}g \tag{15}$$

where B denotes bandwidth required for transmission in [Hz].

By rewriting $\ln(1+g)$ as a Meijer's G-function $G_{2,2}^{1,2}\left(g\middle|\begin{matrix}1,1\\1,0\end{matrix}\right)$ using equation (8.4.6/5) from [32], and substituting the identity and (10) into (15), we get the following expression:

$$\left[\frac{\langle C\rangle_{\mathrm{ora}}}{B}\right] = \frac{1}{2^r}\sum_{k=1}^{\beta} b_k\int_0^{\infty} g^{-1}G_{2,2}^{1,2}\left(g\middle|\begin{matrix}1,1\\1,0\end{matrix}\right) \times G_{1,3}^{3,0}\left(\eta(g)^{\frac{1}{r}}\middle|\begin{matrix}\xi^2+1\\ \xi^2,\alpha,k\end{matrix}\right)\mathrm{d}g \tag{16}$$

For IM/DD, the integral from previous expression is solved by using equation (2.24.1/1) from [32], while for heterodyne detection, the integral from expression (16) is solved by using equation (07.34.21.0013.01) from [33]. By applying these solutions we obtain the closed-form expressions for ORA adaptive transmission algorithm

$$\left[\frac{\langle C\rangle_{\mathrm{ora}}}{B}\right]_{\mathrm{Het}} = \frac{1}{2}\sum_{k=1}^{\beta} b_k G_{3,5}^{5,1}\left(\eta\middle|\begin{matrix}0,1,\xi^2+1\\ \xi^2,\alpha,k,0,0\end{matrix}\right) \tag{17}$$

$$\left[\frac{\langle C\rangle_{\mathrm{ora}}}{B}\right]_{\mathrm{DD}} = \frac{2^{\alpha}}{16\pi}\sum_{k=1}^{\beta} 2^k b_k G_{4,8}^{8,1}\left(\frac{\eta^2}{16}\middle|\begin{matrix}\Xi_{\mathrm{ora}}\\ \Theta_{\mathrm{ora}}\end{matrix}\right) \tag{18}$$

where $\Theta_{\mathrm{ora}} = \{\frac{\xi^2}{2}, \frac{\xi^2+1}{2}, \frac{\alpha}{2}, \frac{\alpha+1}{2}, \frac{k}{2}, \frac{k+1}{2}, 0, 0\}$, and $\Xi_{\mathrm{ora}} = \{0, 1, \frac{\xi^2+1}{2}, \frac{\xi^2+2}{2}\}$, and

$$b_k = \frac{\xi^2 A}{\ln 2}\, a_k\left(\frac{\gamma\beta+\Omega'}{\alpha\beta}\right)^{\frac{\alpha+k}{2}} \tag{19}$$

Equations (17) and (18) can be approximated for high SNR values by using equation (46) as explained in Appendix 3. Results of approximation of these expressions are presented in Figs. 2–7.

4.2 Optimal power and rate adaption

In the OPRA algorithm, the power level and rate parameters vary in response to the changing channel conditions. With this adaptive transmission policy, more power and higher data rates are allocated when the channel condition is good, and the transmission is terminated when the received SNR falls below a cut-off level g_0. OPRA is not suitable for all applications because there are some applications that require fixed rate. Channel capacity for OPRA adaptive algorithm is given as [31]

$$\langle C\rangle_{\mathrm{opra}} = B\int_{g_0}^{\infty}\log_2\left(\frac{g}{g_0}\right)f_g(g)\mathrm{d}g \tag{20}$$

Cut-off level must satisfy condition

$$\int_{g_0}^{\infty}\left(\frac{1}{g_0}-\frac{1}{g}\right)f_g(g)\mathrm{d}g = 1 \tag{21}$$

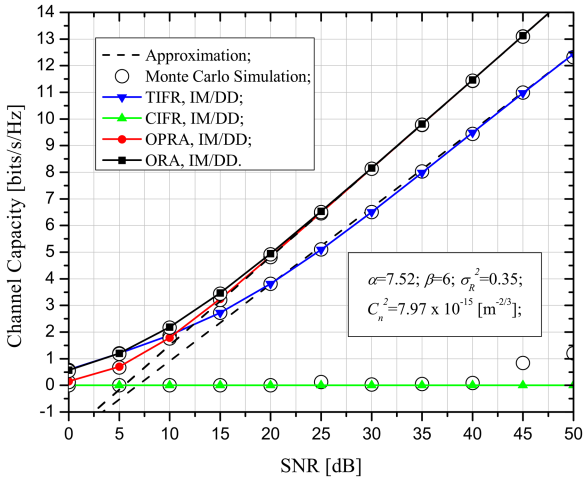

Fig. 2 *Capacity for adaptive transmission algorithms over weak turbulence for IM/DD*

© The Institution of Engineering and Technology 2019

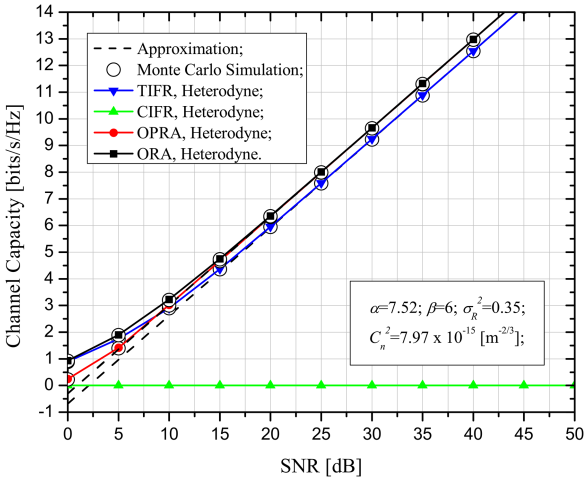

Fig. 3 *Capacity for adaptive transmission algorithms over weak turbulence for heterodyne detection*

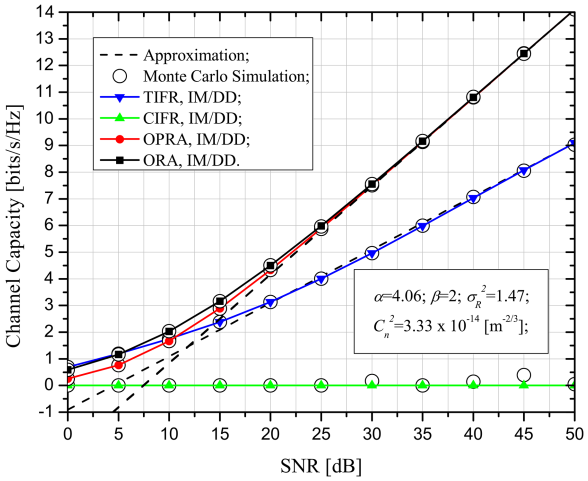

Fig. 4 *Capacity and capacity approximation for adaptive transmission algorithms over moderate turbulence for IM/DD*

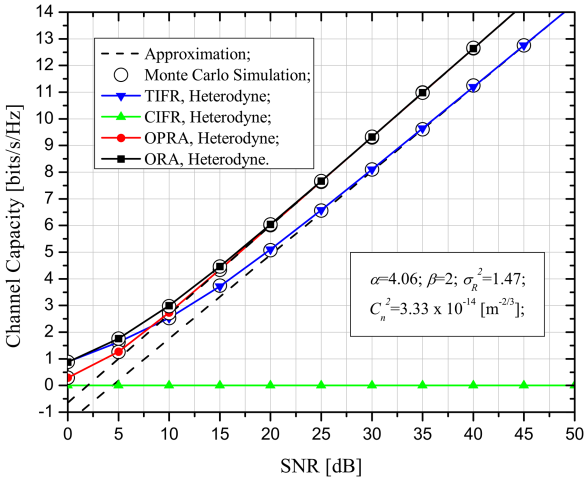

Fig. 5 *Capacity and capacity approximation for adaptive transmission algorithms over moderate turbulence for heterodyne detection*

Expression (20) can be represented as

$$\frac{\langle C\rangle_{\text{opra}}}{B} = \frac{1}{\ln 2}(I_1 - I_2) \tag{22}$$

where $I_1 = \int_{g_0}^{\infty} \ln(g) f_g(g)\mathrm{d}g$ and $I_2 = \int_{g_0}^{\infty} \ln(g_0) f_g(g)\mathrm{d}g$. After solving integrals I_1 and I_2, as derived in Appendix 1, and

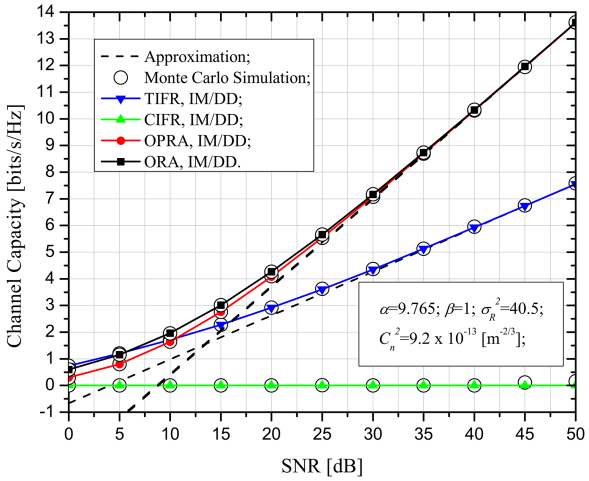

Fig. 6 *Capacity and simulation results for adaptive transmission algorithms over strong turbulence for IM/DD*

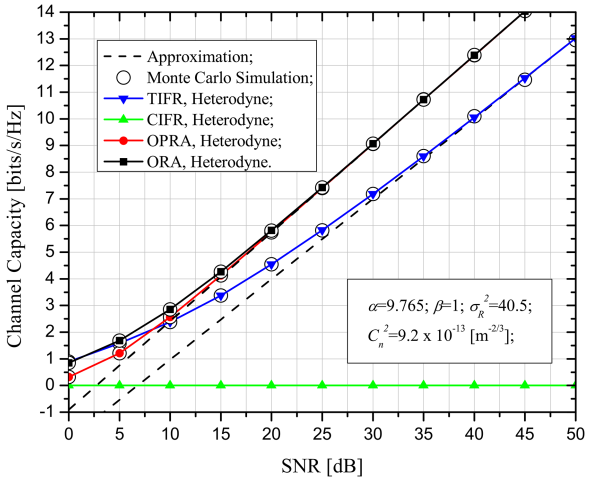

Fig. 7 *Capacity and simulation results for adaptive transmission algorithms over strong turbulence for heterodyne detection*

substituting into (22), we obtain $\langle C\rangle_{\text{opra}}$ for both types of detection, heterodyne and IM/DD

$$\begin{aligned}\left[\frac{\langle C\rangle_{\text{opra}}}{B}\right]_{\text{Het}} = -\sum_{k=1}^{\beta} b_k\Bigg[&G_{3,5}^{4,1}\left(\eta g_0\middle|\begin{matrix}1,\xi^2+1,1\\0,\xi^2,\alpha,k,0\end{matrix}\right)\\&+\ln(g_0)G_{2,4}^{3,1}\left(\eta g_0\middle|\begin{matrix}1,\xi^2+1\\\xi^2,\alpha,k,0\end{matrix}\right)\\&+\ln(g_0)G_{2,4}^{4,0}\left(\eta g_0\middle|\begin{matrix}\xi^2+1,1\\0,\xi^2,\alpha,k\end{matrix}\right)\Bigg]\end{aligned} \tag{23}$$

$$\begin{aligned}\left[\frac{\langle C\rangle_{\text{opra}}}{B}\right]_{\text{DD}} = -\sum_{k=1}^{\beta} b_k\Bigg\{\Bigg[&G_{3,5}^{4,1}\left(\eta g_0\middle|\begin{matrix}1,\xi^2+1,1\\0,\xi^2,\alpha,k,0\end{matrix}\right)\\&+\ln(g_0)G_{2,4}^{3,1}\left(\eta g_0\middle|\begin{matrix}1,\xi^2+1\\\xi^2,\alpha,k,0\end{matrix}\right)\Bigg]\\&+\frac{\ln(g_0)}{16\pi}2^{\alpha+k}G_{3,7}^{7,0}\left(\frac{\eta^2}{16}g_0\middle|\begin{matrix}\Xi_{\text{opra}}\\\Theta_{\text{opra}}\end{matrix}\right)\Bigg\},\end{aligned} \tag{24}$$

where

$$\Theta_{\text{opra}} = \left\{\frac{\xi^2}{2}, \frac{\xi^2+1}{2}, \frac{\alpha}{2}, \frac{\alpha+1}{2}, \frac{k}{2}, \frac{k+1}{2}, 0\right\} \quad \text{and} \quad \Xi_{\text{opra}} = \left\{\frac{\xi^2+1}{2}, \frac{\xi^2+2}{2}, 1\right\}.$$

© The Institution of Engineering and Technology 2019

Table 1 Turbulence conditions and parameters

Parameter	Weak	Moderate	Strong
C_n^2 [m$^{-2/3}$]	$7.97 \cdot 10^{-15}$	$3.33 \cdot 10^{-14}$	$9.2 \cdot 10^{-13}$
σ_R^2	0.35	1.47	40.5
α	7.52	4.06	9.765
β	6	2	1

Equations (23) and (24) can be approximated for high SNR values using Appendix 3. Results of approximation of these expressions are presented in Figs. 2–7.

4.3 Channel inversion with fixed rate

Under this adaptive transmission algorithm, the transmitter adapts the transmit power according to the channel effects state in order to maintain a constant SNR at the receiver, i.e. inverts the channel effects while maintaining a constant transmission rate. CIFR algorithm generally achieves what is known as the outage capacity of the system; that is the maximum constant data rate that can be supported for all channel conditions with some probability of outage [24, 31]

$$\langle C\rangle_{\text{cifr}} = B\log_2\left[1+\frac{1}{\int_0^\infty g^{-1}f_g(g)\mathrm{d}g}\right] \tag{25}$$

After detailed inspection and calculation it was determined that the integral from expression (25) diverges and CIFR $\to$ 0. Regardless of the strength of atmospheric turbulence, the CIFR adaptive transmission algorithm cannot be applied when we have a Málaga atmospheric turbulence model with pointing error. This result was confirmed by the Monte-Carlo simulation (shown in Figs. 2–7). Detailed explanation is given in Appendix 2.

4.4 Truncated channel inversion with fixed rate

Since the CIFR algorithm may exhibit a large channel capacity penalty, or is not feasible at all, a modified channel inversion algorithm is proposed where only the transmitted power is adapted according to the channel state provided that the received SNR is above a certain cut-off SNR g_0 [24], resulting in

$$\langle C\rangle_{\text{tifr}} = B\log_2\left[1+\frac{1}{\int_{g0}^\infty g^{-1}f_g(g)\mathrm{d}g}\right](1-P_{\text{out}}) \tag{26}$$

where P_{out} represents outage probability, defined as: $P_{\text{out}} = \int_0^{g0} f_g(g)\mathrm{d}g$. Integrals and P_{out} from equation (26) can be solved by using equations (07.34.21.0085.01) and (07.34.21.0084.01) from [33].

For heterodyne detection we obtain

$$\left[\frac{\langle C\rangle_{\text{tifr}}}{B}\right]_{\text{Het}} = \log_2\left(1+\frac{2g_0}{I_{(\text{Het})}}\right)(1-P_{(\text{Het})}) \tag{27}$$

where

$$I_{(\text{Het})} = \ln(2)\sum_{k=1}^{\beta} b_k G_{2,4}^{4,0}\left(\eta g_0\middle|\begin{matrix}\xi^2+1, 2\\ 1, \xi^2, \alpha, k\end{matrix}\right) \tag{28}$$

$$P_{(\text{Het})} = \frac{\ln(2)}{2}\sum_{k=1}^{\beta} b_k G_{2,4}^{3,1}\left(\eta g_0\middle|\begin{matrix}1, \xi^2+1\\ \xi^2, \alpha, k, 0\end{matrix}\right) \tag{29}$$

For IM/DD we obtain

$$\left[\frac{\langle C\rangle_{\text{tifr}}}{B}\right]_{\text{DD}} = \log_2\left(1+\frac{g_0}{I_{(\text{DD})}}\right)(1-P_{(\text{DD})}) \tag{30}$$

where

$$I_{(\text{DD})} = \frac{2^\alpha \ln(2)}{16\pi}\sum_{k=1}^{\beta} 2^k b_k G_{3,7}^{7,0}\left(\frac{\eta^2}{16}g_0\middle|\begin{matrix}\Xi_{\text{Itifr}}\\ \Theta_{\text{Itifr}}\end{matrix}\right) \tag{31}$$

where we have denoted

$$\Theta_{\text{Itifr}} = \left\{1, \frac{\xi^2}{2}, \frac{\xi^2+1}{2}, \frac{\alpha}{2}, \frac{\alpha+1}{2}, \frac{k}{2}, \frac{k+1}{2}\right\} \quad \text{and} \quad \Xi_{\text{Itifr}} = \left\{\frac{\xi^2+1}{2}, \frac{\xi^2+2}{2}, 2\right\}.$$

We also have

$$P_{(\text{DD})} = \frac{2^\alpha \ln(2)}{16\pi}\sum_{k=1}^{\beta} 2^k b_k G_{3,7}^{6,1}\left(\frac{\eta^2}{16}g_0\middle|\begin{matrix}\Xi_{\text{Ptifr}}\\ \Theta_{\text{Ptifr}}\end{matrix}\right) \tag{32}$$

where

$$\Theta_{\text{Ptifr}} = \left\{\frac{\xi^2}{2}, \frac{\xi^2+1}{2}, \frac{\alpha}{2}, \frac{\alpha+1}{2}, \frac{k}{2}, \frac{k+1}{2}, 0\right\} \quad \text{and} \quad \Xi_{\text{Ptifr}} = \left\{1, \frac{\xi^2+1}{2}, \frac{\xi^2+2}{2}\right\}.$$

Equations (27) and (30) can also be approximated for high SNR values by using the procedure outlined in Appendix 3. Results of approximation of these expressions are presented in Figs. 2–7.

5 Numerical results and discussion

In order to discuss the use of adaptation techniques, numerically obtained results are also presented graphically. Results of approximate high-SNR expressions for ORA, OPRA and TIFR adaptive transmission algorithms in case of moderate turbulence scenario for IM/DD and heterodyne detection are also graphically presented. Furthermore, the obtained results are confirmed by Monte-Carlo simulations. The simulation results are presented graphically in the case of strong turbulence scenario for IM/DD and heterodyne detection.

In this section, we compare average capacity for FSO communication over Málaga atmospheric turbulence channel with pointing error and path loss for IM/DD and heterodyne detection by using ORA, OPRA, CIFR and TIFR algorithms for adaptive transmission. For the analysed adaptive transmission algorithms, we compare the average capacity for different strengths of atmospheric turbulence. Following parameters are assumed for FSO link: link length $L = 1$ km, wavelength $\lambda = 785$ nm, $\Omega = 1.3265$, $b_0 = 0.1079$, $\rho = 0.596$. Parameters used for weak, moderate and strong turbulence regimes are listed in Table 1.

Numerical results represent ensemble averages obtained by evaluating derived analytical forms, while the simulation uses direct averaging of N independent channel realizations. Simulation procedure uses inverse transform sampling to generate the realisations of Málaga channel with pointing errors corresponding to (10).

Fig. 2 represents capacity for adaptive transmission algorithms over weak turbulence for IM/DD. Fig. 3 represents capacity for adaptive transmission algorithm over weak turbulence for heterodyne detection. Both figures show that there is a higher capacity available when using ORA and OPRA algorithms. Capacity of channel inversion is less than that of ORA and OPRA algorithms. Same applications may require constant rate transmission and reduced complexity at a cost of decreased capacity. TIFR algorithm has less capacity than ORA and OPRA. From the presented figures it can also be seen that higher channel capacity is achieved for heterodyne detection. For example, at SNR of 40 dB, the ORA capacity is 11.4 bits/s/Hz for IM/DD. For same value of SNR and heterodyne detection, ORA capacity is 12.9 bits/s/Hz.

Fig. 4 represents capacities and their high-SNR approximations for adaptive transmission algorithms over moderate turbulence for

© The Institution of Engineering and Technology 2019

IM/DD. Fig. 5 represents capacities and their approximate values for adaptive transmission algorithms with heterodyne detection over moderate turbulence. For both types of detection, shown in Figs. 4 and 5, capacity decreases with increased turbulence strength. Also, higher capacity is achieved for heterodyne detection. Increasing turbulence strength has more influence on TIFR algorithm than on ORA and OPRA algorithms. Also, Figs. 4 and 5 show that the results of the approximations for higher SNR values are in good agreement with the obtained analytical results.

Fig. 6 represents capacities and corresponding Monte-Carlo simulations results for adaptive transmission algorithm over strong turbulence for IM/DD. The analogous results for heterodyne detection are shown in Fig. 7. Strong turbulence affects both types of detection for all considered adaptive transmission algorithms, resulting in lower channel capacities. In all presented figures we observe that the performance gap between different adaptive transmission algorithms decreases with decreasing turbulence strength. For example, we consider TIFR algorithm with heterodyne detection for SNR of 40 dB, resulting in capacity of 12.54 bits/s/Hz for weak turbulence, 11.19 bits/s/Hz for moderate turbulence and 10.048 bits/s/Hz for strong turbulence. Similarly, if we consider strong turbulence and IM/DD, we can achieve capacity of 4 bits/s/Hz for 18.7 dB of SNR when using ORA, 20 dB when using OPRA, and 27.5 dB when using TIFR. When using heterodyne detection in the same turbulence conditions, the same capacity level is achieved for 13.7, 14 and 17.5 dB when employing ORA, OPRA and TIFR algorithms, respectively.

We have encountered a difficulty in simulation procedure when trying to confirm zero-capacity of CIFR transmission with heterodyne detection. Let N denote the number of independent simulation runs. By increasing N one should expect to obtain the results that are progressively in closer agreement with analytical results. However, there are cases where the required number of simulation runs is higher than practically feasible. One such example is the CIFR adaptive transmission for the case of heterodyne detection considered in this paper (see Fig. 7). By examining closely the cumulative distribution function of the random variable involved, we notice that for average SNR of 50 dB and number of simulation runs of $N = 10^6$, we can rarely expect any realisations of random variable that are lower than -10 dB. Cumulative probability that the SNR falls below this threshold level is about 10^{-6}, i.e. approximately $1/N$. On the other hand, the obtained simulation dataset is equivalent of CIFR adaptation excluding realisations below the -10 dB threshold, since we almost never get any. Even if we increase the number of simulation runs to 10^{12}, we would only be able to account for realisations above -70 dB in this example, which is still not adequate to demonstrate close agreement with analytical results. Accurate simulation of such processes requires advanced simulation techniques which are not considered here further. Therefore, the perceived SNR threshold in our simulations decreases as $1/N$ for the heterodyne case. When considering IM/DD systems, the problem is easily overcome with increasing the number of simulation runs, as the perceived threshold decreases with $1/N^2$.

6 Conclusion

We have investigated capacity for FSO communication over Málaga atmospheric turbulence channel with pointing error and path loss for IM/DD and heterodyne detection.

Analytical expression in closed form for ORA, OPRA and TIFR adaptive transmission algorithms are derived. We show that it is not possible to achieve any definitive channel capacity when using CIFR adaptive transmission algorithm over the proposed channel model. For the proposed model of atmospheric turbulence (for both types of detection and for different atmospheric turbulence strengths), channel capacity of CIFR adaptive transmission algorithm tends to zero. Obtained results are numerically evaluated and graphically presented for different strength of atmospheric turbulence (weak, moderate and strong) and for both types of detection (IM/DD and heterodyne).

Results of asymptotic high-SNR approximate expressions for ORA, OPRA and TIFR adaptive transmission algorithms are graphically presented for the case of moderate turbulence scenario and both detection types. Also, the obtained results are confirmed by Monte-Carlo simulations. The simulation results are graphically presented for the case of strong turbulence scenario, for IM/DD and heterodyne detection.

We have shown that heterodyne detection is better than IM/DD and provides greater reliability and capacity for all proposed turbulence scenarios. Although heterodyne detection has better performance, IM/DD is more often used in commercial systems due to its simple design.

ORA and OPRA adaptive transmission algorithms allow higher channel capacities when compared to TIFR algorithm. The advantage of ORA and OPRA algorithms is in their flexibility that allows control of data rate by adjusting the power of the transmitter. By increasing or decreasing the transmitted power, we have an additional degree of freedom to increase or decrease the data rate. On the other hand, TIFR algorithm is applied in systems that require constant data transfer rate so it is not possible to perform rate adaptation as in ORA and OPRA algorithms. The main advantage of fixed-rate algorithms is their simple implementation, regardless of the fact that they exhibit lower values of channel capacity. Also, we note that turbulence strength has more significant effect on TIFR algorithm than it has on ORA and OPRA.

7 Acknowledgments

This paper is supported by Ministry of Education, Science and Technological Development of the Republic of Serbia, under projects TR-32051 and III-44006. Last author is funded by the framework of Competitiveness Enhancement Program of the National Research Tomsk Polytechnic University, Russia.

8 References

[1] Hranilovic, S.: '*Wireless optical communication systems*' (Springer, New York, 2005)

[2] Arnon, S., Barry, J.R., Karagiannidis, G.K., *et al.*: '*Advanced optical wireless communication systems*' (Cambridge University Press, Cambridge UK, 2012)

[3] Andrews, L.C., Phillips, R.L.: '*Laser beam propagation through random media*' (SPIE, Bellingham WA, USA, 2005)

[4] Willebrand, H., Ghuman, B.S.: '*Free space optics: enabling optical connectivity in today's networks*' (SAMS, Indianopolis USA, 2002)

[5] Lapidoth, A., Moser, S.M., Wigger, M.A.: 'On the capacity of free-space optical intensity channels', *IEEE Trans. Inf. Theory*, 2009, **55**, (10), pp. 4449–4461

[6] Al-Habash, M.A., Andrews, L.C., Phillips, R.L.: 'Mathematical model for the irradiance probability density function of a laser beam propagating through turbulent media', *Opt. Eng.*, 2001, **40**, (8), pp. 1554–1562

[7] Garrido-Balsells, J.M., Jurado-Navas, A., Paris, J.F., *et al.*: 'Novel formulation of the m model through the generalized – k distribution for atmospheric optical channels', *Opt. Express*, 2015, **23**, (5), pp. 6345–6358

[8] Garrido-Balsells, J.M., Lopez-Martinez, F.J., Castillo-Vázquez, M., *et al.*: 'Performance analysis of FSO communications under los blockage', *Opt. Express*, 2017, **25**, (21), pp. 12550–12562

[9] Simon, M.K., Alouini, M.S.: '*Digital communication over fading channels*' (John Wiley & Sons Inc., Hoboken, NJ, 2005)

[10] Jurado–Navas, A., Maria, J., Francisco, J., *et al.*: 'A unifying statistical model for atmospheric optical scintillation', in Awrejcewicz, Jan (Eds.): '*Numerical simulations of physical and engineering processes*' (InTech, Croatia, 2011), pp. 181–206

[11] Alheadary, W.G., Park, H.K., Alouini, M.S.: 'Performance analysis of subcarrier intensity modulation using rectangular QAM over Malaga turbulence channels with integer and non-integer β', *Wirel. Commun. Mob. Comput.*, 2016, **16**, pp. 2730–2742

[12] López-González, F.J., Jurado-Navas, A., Garrido-Balsells, J.M., *et al.*: 'Characterization of sub-channel based Málaga atmospheric optical links with real β parameter', *Opt. Appl.*, 2017, **XLVII**, (4), pp. 545–556

[13] Ansari, I.S., Yilmaz, F., Alouini, M.S.: 'Performance analysis of free-space optical links over málaga (m) turbulence channels with pointing errors', *IEEE Trans. Wirel. Commun.*, 2016, **15**, (1), pp. 91–102

[14] Amirabadi, M.A., Tabataba Vakili, V.: 'A new optimization problem in FSO communication system', *IEEE Commun. Lett.*, 2018, **22**, (7), pp. 1442–1445

[15] Amirabadi, M.A., Tabataba Vakili, V.: 'A novel hybrid FSO/RF communication system with receive diversity', *Signal Process.*, 2018, pp. 1–5. Available at http://arxiv.org/abs/1802.07348

[16] Balaji, K.A., Prabu, K.: 'Performance evaluation of FSO system using wavelength and time diversity over Malaga turbulence channel with pointing errors', *Opt. Commun.*, 2018, **410**, pp. 643–651

[17] Chen, L., Wang, W.: 'Multi-diversity combining and selection for relay-assisted mixed RF/FSO system', *Opt. Commun.*, 2017, **405**, pp. 1–7

© The Institution of Engineering and Technology 2019

[18] Nguyen, N.T.T., Vu, M.Q., Pham, H.T.T., *et al.*: 'Performance enhancement of HAP-based relaying M-PPM FSO system using spatial diversity and heterodyne detection receiver', *J. Opt. Commun.*, 2018, pp. 1–10
[19] Ansari, I.S., Alouini, M.S., Cheng, J.: 'Ergodic capacity analysis of free-space optical links with nonzero boresight pointing errors', *IEEE Trans. Wirel. Commun.*, 2015, **14**, (8), pp. 4248–4264
[20] Nistazakis, H.E., Karagianni, E.A., Tsigopoulos, A.D., *et al.*: 'Average capacity of optical wireless communication systems over atmospheric turbulence channels', *J. Lightwave Technol.*, 2009, **27**, (8), pp. 974–979
[21] Peppas, K.P., Stassinakis, A.N., Topalis, G.K., *et al.*: 'Average capacity of optical wireless communication systems over I-K atmospheric turbulence channels', *J. Opt. Commun. Netw.*, 2012, **4**, (12), pp. 1026–1032
[22] Nistazakis, H.E., Tombras, G.S., Tsigopoulos, A.D., *et al.*: 'Capacity estimation of optical wireless communication systems over moderate to strong turbulence channels', *Journal of Communications and Networks*, 2009, **11**, (4), pp. 384–389
[23] Peppas, K.P., Stassinakis, A.N., Nistazakis, H.E., *et al.*: 'Capacity analysis of dual amplify-and-forward relayed free-space optical communication systems over turbulence channels with pointing errors', *J. Opt. Commun. Netw.*, 2013, **5**, (9), pp. 1032–1042
[24] Hassan, M.Z., Hossain, M.J., Cheng, J.: 'Ergodic capacity comparison of optical wireless communications using adaptive transmissions', *Opt. Express*, 2013, **21**, (17), pp. 20346–20362
[25] Anees, S., Bhatnagar, M.R.: 'Information theoretic analysis of a dual-hop fixed gain af based mixed RF-FSO system'. 2015 IEEE 26th Annual Int. Symp. on Personal, Indoor, and Mobile Radio Communications (PIMRC), Hong Kong, 2015, pp. 927–931
[26] Gappmair, W.: 'Further results on the capacity of free-space optical channels in turbulent atmosphere', *IET Commun.*, 2011, **5**, (9), pp. 1262–1267
[27] Kikuchi, K.: '*High spectral density optical communication technologies*' (Springer, Berlin, Heidelberg, 2010)
[28] Andrews, L.C., Phillips, R.L., Young, C.Y.: '*Laser beam scintillation with applications*' (SPIE, WA, 2001)
[29] Petković, M.I., Djordjević, G.T., Milić, D.N.: 'Ber performance of IM/DD FSO system with ook using apd receiver', *Radioengineering*, 2014, **23**, (1), pp. 480–487
[30] Petković, M., Djordjević, G.T: 'Average BER of dual-branch FSO system employing sim-bpsk influenced by Malaga atmospheric turbulence with pointing errors'. Proc. of 4th Int. Conf. on Electrical,Electronics and Computing Engineering,(IcETRAN 2017). (Society for Electronics, Telecommunications, Computers, Automatic Control and Nuclear Engineering), Kladovo, 2017, pp. TEI1.4.1–TEI1.4.6
[31] Stefanović, M.Č., Anastasov, J.A., Panić, S.R., *et al.*: 'Channel capacity analysis under various adaptation policies and diversity techniques over fading channels', in Ali, Eksim (Eds.): '*Wireless communications and networks - recent advances*' (InTech, Croatia, 2012), pp. 281–302
[32] Prudnikov, A.P., Brychkov, J.A.: '*Integrasl and series*' (Fizmatlit, Moscow, 2003)
[33] W.R. Inc.: 'Wolfram functions site'. (Wolfram Research, Inc., 2019. Available at: http://functions.wolfram.com

9 Appendix

9.1 Appendix 1: OPRA adaptive transmission algorithm

Integral $I_1 = \int_{g_0}^{\infty} \ln(g) f_g(g) \mathrm{d}g$ for OPRA is somewhat complicated to solve. It consists of $1/g$, logarithm function, and Meijer's G-function, from combining equations (10) and (20). We solve this integral using the partial integration method $\int_a^b u\mathrm{d}v = (uv)|_a^b - \int_a^b v\mathrm{d}u$ where we take $u = \ln(g)$ and $\mathrm{d}v = \frac{1}{g} G_{1,3}^{3,0}\left(\eta g^{\frac{1}{r}} \middle| \begin{matrix} \xi^2+1 \\ \xi^2, \alpha, k \end{matrix}\right)\mathrm{d}g$.

For IM/DD and heterodyne detection, antiderivative v is obtained using equation (07.34.21.0003.01) from [33]

$$v = G_{2,4}^{3,1}\left(\eta g \middle| \begin{matrix} 1, \xi^2+1 \\ \xi^2, \alpha, k, 0 \end{matrix}\right) \tag{33}$$

First term in partial integration rule is

$$(uv)|_a^b = \left(\ln(g) G_{2,4}^{3,1}\left(\eta g \middle| \begin{matrix} 1, \xi^2+1 \\ \xi^2, \alpha, k, 0 \end{matrix}\right)\right)\Big|_{g_0}^{\infty}$$

For $g \to \infty$, we apply the L' Hopital's rule, yielding

$$I_{11} = \lim_{g \to \infty} \left(\ln(g) G_{2,4}^{3,1}\left(\eta g \middle| \begin{matrix} 1, \xi^2+1 \\ \xi^2, \alpha, k, 0 \end{matrix}\right)\right) = 0, \tag{34}$$

and we write: $I_{12} = \ln(g_0) G_{2,4}^{3,1}\left(\eta g_0 \middle| \begin{matrix} 1, \xi^2+1 \\ \xi^2, \alpha, k, 0 \end{matrix}\right)$, for $g = g_0$. Second term in partial integration equals

$$\int_a^b v\mathrm{d}u = \int_{g_0}^{\infty} g^{-1} G_{2,4}^{3,1}\left(\eta g \middle| \begin{matrix} 1, \xi^2+1 \\ \xi^2, \alpha, k, 0 \end{matrix}\right)\mathrm{d}g \tag{35}$$

We solve this integral using equation (2.24.2/3) from [32]

$$I_{13} = G_{3,5}^{4,1}\left(\eta g_0 \middle| \begin{matrix} 1, \xi^2+1, 1 \\ 0, \xi^2, \alpha, k, 0 \end{matrix}\right) \tag{36}$$

Integral I_1 therefore equals $I_1 = \sum_{k=1}^{\beta} b_k (I_{11} - I_{12} - I_{13})$. Integral $I_2 = \ln(g_0) \int_{g_0}^{\infty} f_g(g)\mathrm{d}g$ is solved using (07.34.21.0085.01) from [33], yielding

$$I_{2(DD)} = \frac{\ln(g_0)}{16\pi} \sum_{k=1}^{\beta} b_k 2^{\alpha+k} G_{3,7}^{7,0}\left(\frac{\eta^2}{16} g_0 \middle| \begin{matrix} \Xi_{\mathrm{opra}} \\ \Theta_{\mathrm{opra}} \end{matrix}\right) \tag{37}$$

$$I_{2(\mathrm{Het})} = \ln(g_0) \sum_{k=1}^{\beta} b_k G_{2,4}^{4,0}\left(\eta g_0 \middle| \begin{matrix} \xi^2+1, 1 \\ 0, \xi^2, \alpha, k \end{matrix}\right) \tag{38}$$

Final closed-form expressions for OPRA adaptive transmission algorithms are given in Section (4.2).

9.2 Appendix 2: CIFR adaptive transmission algorithm

To determine the capacity of CIFR transmission, we need to evaluate the following expression:

$$\int_0^{+\infty} \frac{1}{x} f_g(x)\,\mathrm{d}x, \tag{39}$$

where $f_g(x)$ corresponds to (10). Results of Monte-Carlo simulations indicate that the value diverges, but we are set to formally prove so. Since there are multiple summands if $\beta > 1$, we need to prove that at least one of them

$$\int_0^{+\infty} \frac{1}{x^2} G_{30}^{13}\left(\eta x^{1/r} \middle| \begin{matrix} \xi^2+1 \\ \xi^2, \alpha, k \end{matrix}\right)\mathrm{d}x \tag{40}$$

diverges for the specified k. The constants that are non-essential for integration are neglected. Simple change of variable allows the scaling factor η to be left out, and we further concentrate on the case of $k = 1$. The improper integral has a singular point $x = 0$ that presents a problem for integration. Therefore, we want to prove that the integral diverges in arbitrary small ϵ-neighbourhood of the singularity

$$J = \int_0^{\epsilon} \frac{1}{x^2} G_{1,3}^{3,0}\left(x^{1/r} \middle| \begin{matrix} \xi^2+1 \\ \xi^2, \alpha, 1 \end{matrix}\right)\mathrm{d}x \to +\infty \tag{41}$$

We first notice that the following limit exists:

$$\lim_{x \to 0^+} \frac{1}{x^{1/r}} G_{1,3}^{3,0}\left(x^{1/r} \middle| \begin{matrix} \xi^2+1 \\ \xi^2, \alpha, 1 \end{matrix}\right) = \frac{\Gamma(\alpha-1)}{\xi^2-1} \tag{42}$$

Furthermore, if the function under the limit operator monotonically decreases with x, we can simply use the comparison test to write

$$\frac{\Gamma(\alpha-1)}{\xi^2-1} \int_0^{\epsilon} \frac{\mathrm{d}x}{x^{2-1/r}} \geq J \geq \frac{G_{1,3}^{3,0}\left(\epsilon^{1/r} \middle| \begin{matrix} \xi^2+1 \\ \xi^2, \alpha, 1 \end{matrix}\right)}{\epsilon^{1/r}} \int_0^{\epsilon} \frac{\mathrm{d}x}{x^{2-1/r}} \tag{43}$$

© The Institution of Engineering and Technology 2019

Since the p-integrals in the above inequality diverge for $r \geq 1$, this would be enough to prove that J also diverges. In the case of monotonically increasing function, we get similar inequality with the sense of comparison operators reversed, and the same outcome that J diverges. Thus, we prove that CIFR adaptive transmission in the strict sense is not feasible for the analysed system model.

9.3 Appendix 3: Approximate capacity for high SNR

Analytical expressions for the channel capacities of ORA, OPRA and TIFR adaptive transmission algorithms for IM/DD and heterodyne detection are presented in (17), (18), (23), (24), (27) and (30). Moreover, these expressions can be closely approximated by simpler ones for high SNR values. We start the procedure by finding the derivative of Meijer G function with respect to SNR

$$k = \frac{\mathrm{d}}{\mathrm{d}\,\mathrm{SNR}}\left\{G_{p,q}^{m,n}\left(C_0 \cdot 10^{-\frac{\mathrm{SNR}}{10}}\middle|\begin{matrix}a_1, \ldots, a_p\\ b_1, \ldots, b_q\end{matrix}\right)\right\}, \tag{44}$$

where

$$C_0 = \frac{1}{c}\left(\frac{\alpha\beta\kappa(\gamma + \Omega')}{\gamma\beta + \Omega'}\right)^r.$$

By applying simple change of variable $z = C_0 \cdot 10^{-\mathrm{SNR}/10}$, and equation (07.34.20.0002.01) from [33], we express the derivative as

$$k = -\frac{\ln 10}{10} G_{p+1,q+1}^{m,n+1}\left(z\middle|\begin{matrix}0, a_1, \ldots, a_p\\ b_1, \ldots b_m, 1, b_{m+1}, \ldots, b_q\end{matrix}\right) \tag{45}$$

The form of approximate expression for channel capacity is then

$$\frac{\langle C\rangle^{(\mathrm{a})}}{B} = \text{constant} \times (n_0 + k_0 \cdot \mathrm{SNR}_{[\mathrm{dB}]}), \tag{46}$$

where we denote $k_0 = \lim_{z \to 0^+} k$. Parameter n_0 is obtained as

$$n_0 = \lim_{z \to 0^+}\left[G_{p,q}^{m,n}\left(z\middle|\begin{matrix}a_1, \ldots, a_p\\ b_1, \ldots, b_q\end{matrix}\right) + 10\,k_0 \log_{10}\left(\frac{z}{C_0}\right)\right] \tag{47}$$

Approximations of channel capacity are obtained by applying the procedure to (17), (18), (23), (24), (27) and (30). For example, the approximate high-SNR channel capacity of direct-detection ORA transmission becomes

$$\left[\frac{\langle C\rangle_{\mathrm{ora}}}{B}\right]_{\mathrm{DD}} \simeq \left(\sum_{i=1}^{\beta} b_i n_i\right) + \left(\sum_{i=1}^{\beta} b_i k_i\right)\mathrm{SNR}_{[\mathrm{dB}]}, \tag{48}$$

where

$$\begin{aligned} k_i &= \frac{\ln(10)}{10}\frac{1}{2\xi^2}\Gamma(\alpha)\Gamma(i)\\ n_i &= \frac{\Gamma(\alpha)\Gamma(i)}{\xi^2}\left[\ln\left(\frac{\beta\gamma + \Omega'}{\alpha\beta\kappa(\gamma + \Omega')\sqrt{2\pi}}\right)\right.\\ &\quad \left. + \frac{1}{2} - \frac{1}{\xi^2} + \Psi(i) + \Psi(\alpha)\right] \end{aligned} \tag{49}$$

In the above expression for coefficients n_i, symbol $\Psi(\cdot)$ stands for the digamma function defined as (06.14.27.0002.01) in [33].

© The Institution of Engineering and Technology 2019